

Applicability of half-space-based methods to non-conforming elastic normal contact problems

Deng, Xiangyun; Qian, Zhiwei; Li, Zili; Dollevoet, Rolf

DOI

[10.1016/j.ijmecsci.2017.04.002](https://doi.org/10.1016/j.ijmecsci.2017.04.002)

Publication date

2017

Document Version

Accepted author manuscript

Published in

International Journal of Mechanical Sciences

Citation (APA)

Deng, X., Qian, Z., Li, Z., & Dollevoet, R. (2017). Applicability of half-space-based methods to non-conforming elastic normal contact problems. *International Journal of Mechanical Sciences*, 126, 229-234. <https://doi.org/10.1016/j.ijmecsci.2017.04.002>

Important note

To cite this publication, please use the final published version (if applicable). Please check the document version above.

Copyright

Other than for strictly personal use, it is not permitted to download, forward or distribute the text or part of it, without the consent of the author(s) and/or copyright holder(s), unless the work is under an open content license such as Creative Commons.

Takedown policy

Please contact us and provide details if you believe this document breaches copyrights. We will remove access to the work immediately and investigate your claim.

© 2017 Manuscript version made available under CC-BY-NC-ND 4.0 license

<https://creativecommons.org/licenses/by-nc-nd/4.0/>

Postprint of International Journal of Mechanical Sciences

Volume 126, June 2017, Pages 229–234

Link to formal publication (Elsevier): <https://doi.org/10.1016/j.ijmecsci.2017.04.002>

Applicability of half-space-based methods to non-conforming elastic normal contact problems

Xiangyun Deng, Zhiwei Qian, Zili Li* and Rolf Dollevoet

Section of Railway Engineering, Faculty of Civil Engineering and Geosciences, Delft University of Technology, Stevinweg 1, 2628 CN, Delft, the Netherlands

*Corresponding author

E-mail address: Z.Li@tudelft.nl

Abstract

The half-space assumption has been employed in many solution methods for non-conforming contact problems in elasticity such as the Hertz theory and the Kalker's variational theory. It is generally believed that to guarantee acceptable accuracy in these half-space-based methods, the characteristic size (twice length of one semi-axis) of the contact patch should be much smaller than the significant dimensions (i.e. the height, width, length and the principal radii of curvature) of each body in contact. In engineering practice, the 3x rule is often employed, which requires that the significant dimensions be at least three times as large as the characteristic size. However, this requirement has not been justified. In this paper, the applicability of half-space-based methods is investigated by comparing the solutions obtained using the Hertz theory and the Kalker's theory with those of the Finite Element (FE) method which is not limited to the half-space assumption. Different combinations of significant dimensions in terms of height, width and length are studied. Various contact patch eccentricities and contact body shapes are considered. It is found that the half-space-based methods yield high-accuracy calculation for non-conforming contact problems. Even when the significant dimensions are as small as 1.1x the characteristic size, the differences between the solutions of the half-space-based methods and the FE method are within 9%. The findings of this paper indicate that the typically assumed 3x restriction can be greatly relaxed. Since a clear estimation of the deviation of the results of half-space-based methods from those of the FE method is provided, the applicability of half-space-based methods in mechanical engineering can be much better understood.

Keywords: non-conforming elastic contact, half-space assumption, FE method, characteristic size, significant dimensions.

1. Introduction

Contact problems exist in many mechanical systems such as wheel-rail interfaces, bearings, gears, mechanical linkages, and metal forming processes [1, 2]. These problems are related to the analysis of the friction, wear or fatigue failure of the components in contact and require accurate calculations of their stresses and deformations. The study of contact problems was initiated by Hertz [3], who solved the normal problem in which no friction was considered. A classical 2D solution for the frictional rolling contact problem was provided by

Carter [4]. In the 1950s, Johnson [5] presented solutions for the frictional rolling of spheres. Concerning wheel-rail rolling contact, the most popular method is the Kalker's variational theory based on virtual work which is implemented using the Boundary Element Method [6]. This theory enables the treatment of arbitrary creepage and spin. All these theories are based on the half-space assumption. It is considered that this assumption requires that the characteristic size of the contact patch be much smaller than the significant dimensions of the bodies in contact. In the case of an elliptical contact, the characteristic size can be twice the length of one semi-axis. The significant dimensions of the contact bodies can be their width, length or height and/or the principal radii of curvature in the vicinity of the contact patch.

In reality, bodies in contact always have finite dimensions. In many cases, the significant dimensions of the body in contact are close to the characteristic size of the contact patch. Considering switch and crossing panels of railways as an example, the width and the radius of curvature at the crossing nose may be close to the characteristic size of the contact patch [7], as shown in Fig. 1(a). Other examples include asperity contacts (see Fig. 1(b)) [8, 9], bearing contact [10], spherical indentation contact [11] and gears [12]. In these contacts, one or more dimensions may be close to the characteristic size. Half-space-based methods have been widely used to solve these contact problems because such methods are efficient and easy to use. However, the applicability of these methods is questionable when the significant dimensions of the contact bodies are close to the characteristic size of the contact patch. In engineering practice the 3x rule is usually employed [13], which requires that the significant dimensions be at least three times as large as the characteristic size of the contact patch. However, to the authors' knowledge, the literature lacks sufficient justification of such a requirement or any analysis of its accuracy. This paper proposes quantitative criteria for assessing the applicability of the classical half-space-based methods to non-conforming elastic normal contacts by considering the influence of the significant dimensions in the vicinity of the contact patch.

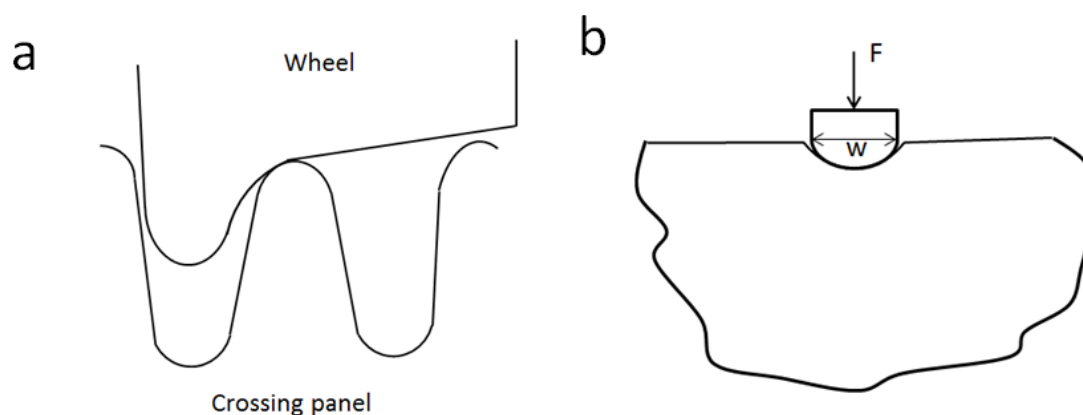


Fig. 1. (a) Wheel-rail contact in the case of a crossing panel [7]; (b) Single asperity contact [8].

In recent years, there have been many studies of various contact mechanical problems in which the real boundary conditions were considered. The Finite Element (FE) method is

commonly used in such studies. One advantage of the FE method is that the half-space assumption is not required. Its computational accuracy was verified several decades ago for static elastic contact problems by Chan and Tuba [14], and recently for frictional rolling contact problems by Zhao and Li [15]. Yan and Fischer [16] compared the contact pressure solution obtained using the FE method with that of the Hertz theory for the case of a standard rail, a crane rail and a switch. They found that the two solutions agreed well as long as the materials were assumed to be linear elastic in nature. Wiest et al. [7] investigated the contact pressure distribution between a wheel and a rail crossing nose using the FE method. They found that the solutions of the FE method and two half-space-based methods were in good agreement even though the radius of curvature at the crossing nose near the contact point was close to the size of the contact patch. In these works, the significant dimension was assumed to be the principal radius of curvature of the contact body, whereas other significant dimensions, such as height, width and length, were not addressed.

In this paper, the FE method is employed to investigate the accuracy and applicability of half-space-based methods. The static normal contact between non-conforming geometrical bodies is studied by comparing the solutions obtained using half-space-based methods with those of the FE method. A number of combinations of different significant dimensions of the contact bodies in terms of height, width and length with various eccentricities of the contact patch (the ratios of the semi-axes of the contact patch) and different shapes of the contact body are considered. The corresponding deviations of the half-space-based methods from the FE method are analyzed, and the critical significant dimensions are determined.

2. Assessment strategy on solution methods for contact problems

In the present work, an FE contact model is built using the software package ANSYS. The Hertz theory and the Kalker's variational theory are chosen for comparison, as they are representative half-space-based methods. The deviations of the results of the half-space-based methods from those of the FE method are analyzed for each significant dimension. Notably, the results computed using the half-space-based methods are independent of the dimensions.

2.1. FE contact model

2.1.1 FE model description

In the FE model, two bodies with cylindrical geometries in static normal contact are considered. Schematic diagrams of the model are shown in Fig. 2. A Cartesian coordinate system $Oxyz$ is created as shown in the figure, of which the origin O is located at the point of initial contact. The upper body is represented by a cylinder. The radius r_A is 460 mm, and the width w_A is 135 mm. The lower body is modeled as a partial cylinder whose cross section is perpendicular to the x axis. The radius of curvature r is 300 mm. Furthermore, cylindrical bodies in contact with other principal radii of curvature and contact bodies with arbitrary geometries are also considered to study the effects of the contact patch eccentricity and of the contact bodies shapes. The height h , the width w and the length l are selected in

accordance with the designs to be discussed in Section 2.2. The lower body is connected to a base whose bottom is fixed.

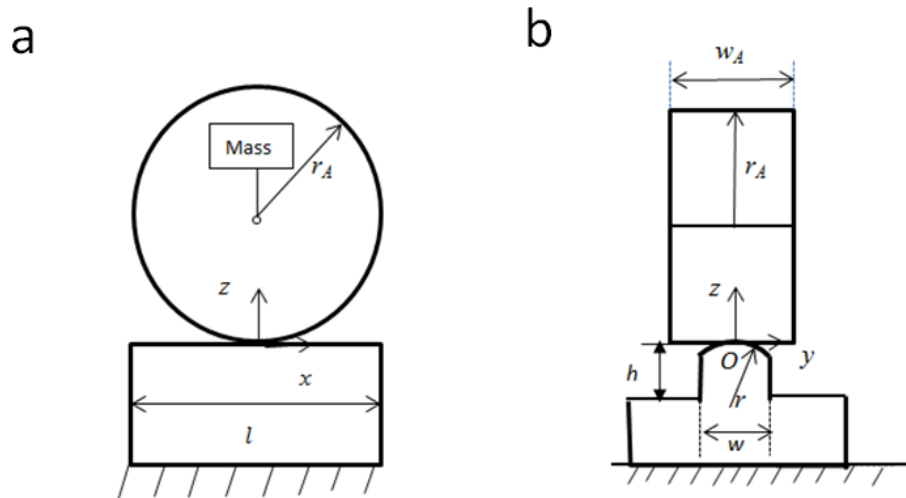


Fig. 2. Schematic diagrams of the FE model: (a) Front view; (b) Side view.

The contact bodies are meshed using 8-node solid elements. A non-uniform mesh is used in the potential contact zone to achieve high solution accuracy at a reasonable computational expense, as shown in Fig. 3. A fine mesh of 0.31 mm is assigned to both the lower body and the upper body in the potential contact zone. A relatively coarse mesh is used for the remaining portions of the bodies.

In the model, elastic material properties are assumed. The Young's modulus is 210 GPa, and the Poisson's ratio is 0.3. A total static vertical load of 86 kN is applied to the upper body.

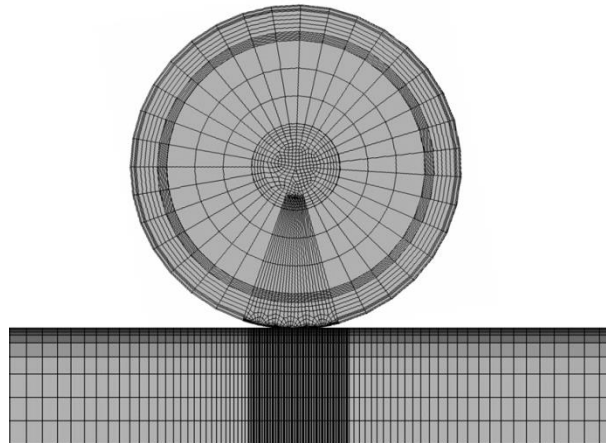


Fig. 3. Mesh of the FE model for static normal contact.

Various contact algorithms are available in ANSYS for studying the static contacts. In this work, the penalty method is used [17] to enforce the contact constraints. In studies of normal contact behavior, frictional contact is not considered, and therefore, no tangential load is applied. The model used in this work is static; thus, it is different from explicit dynamic models such as those in [15]. A static model is used in this work because the intent

is to study the influence of the half-space assumption in half-space-based methods, and dynamic effects are not considered.

2.1.2 Design of the significant dimensions of the lower body

To quantitatively study the accuracy of half-space-based methods and the critical dimensions that most influence their accuracy, solutions for contacts between upper and lower bodies with various significant dimensions are analyzed. The significant dimensions of the lower body are designed based on the size of the contact patch as calculated using the Hertz theory. That is, in the design, the Hertz theory is first applied to compute the reference contact patch, which is elliptical in shape. The parameters a_0 and b_0 denote the reference major and minor semi-axes of the elliptical contact patch in the x and y directions, respectively. The Hertz solution is used as the reference because it can be easily calculated. The significant dimensions of the lower body in the FE model are defined as the height, width and length in the vicinity of the contact patch. Specifically, they are expressed as ratios of each actual dimension over the corresponding dimension of the reference contact patch size ($2b_0$ or $2a_0$). Therefore, the height, width and length are represented by the normalized variables $h/2b_0$, $w/2b_0$ and $l/2a_0$, respectively. The purpose of this normalization is to make this study more general. The normalized width of the lower body is selected to start with 1.1, which is very close to the extreme case of 1.0. Then, the width is varied from 1.1 to 2.0 and 8.0. The width of 8.0 is considered to represent the half-space scenario, as this value indicates a width that is much larger than the characteristic size of the contact patch. The length $l/2a_0$ is set equal to the width $w/2b_0$. For each width, three heights ($h/2b_0$), namely 0.4, 1.0 and 4.0, are considered. These combinations of significant dimensions in terms of height, width and length are investigated for the static normal contact problem.

2.2. The Kalker's variational theory

The theoretical basis and computer implementations of the Kalker's variational theory are described in [6]. A brief introduction to the theory is provided here. The theory follows the variational principle, which states that the stress field within a solid is true when the complementary potential energy is at its minimum value. It is implemented on the basis of the Boundary Element Method. The following assumptions are made. The contact patch is flat and it is small compared with the significant dimensions and the radii of curvatures of the two contact bodies. In addition, the inertial effect is ignored.

In the Cartesian coordinate system $Oxyz$, the contact problem can be expressed in the form of the minimization of complementary energy $C_{u,p}$ in surface mechanical form. It is in terms of the surface tractions, including the normal pressure p_z and the tangential traction p_τ . The expression is [6, 18]

$$\min C_{u,p} = \int_{A_c} \left(h + \frac{1}{2} u_z \right) p_z dS + \int_{A_c} \left(W_\tau + \frac{1}{2} u_\tau - u'_\tau \right) p_\tau dS \quad (1)$$

where $p_z \geq 0$, $|p_\tau| \leq f p_z$ in A_c , f is the friction coefficient, A_c is the potential contact surface area, dS is the elementary area on A_c . h is the undeformed distance between the two contact bodies, u_z is the displacement in the normal direction, W_τ is the rigid body shift,

u_τ denotes the displacement in the tangential direction, u'_τ denotes the tangential displacement at the previous time step.

The contact bodies $\alpha = 1, 2$ are presumed to satisfy the half-space assumption and the material is linear elastic. The relation between the displacement u_i in the direction i at the location x_α (the response point) and the surface traction p_j in the direction j at the location y_α (the impulse point) can be established according to Boussinesq [19] and Cerruti [20], which reads [6]

$$u_i(x_\alpha) = \iint_{A_C} A_{ij}(y_\alpha - x_\alpha) p_j(y_\alpha) dS \quad \alpha = 1, 2; i, j = x, y, z \quad (2)$$

where $A_{ij}(y_\alpha - x_\alpha)$ is the influence function of body α , and it can be determined analytically.

Applying the Boundary Element Method, Equation (1) can be discretized into

$$\begin{aligned} \min C_{p_{JJ}}^* &= \frac{1}{2} p_{Ii} A_{IiJj} p_{Jj} + \{h_J p_{Jz} + (W_{J\tau} - u'_{J\tau}) p_{J\tau}\} \\ \text{sub } p_{Jz} &\geq 0, \quad |p_{J\tau}| \leq f p_{Jz} \end{aligned} \quad (3)$$

where the subscript I, J denotes the uniformly discretized element, the p_{JJ} in $C_{p_{JJ}}^*$ means that the primal variables for the minimization are the independent variables p_{JJ} .

In this work, the normal contact problem without tangential traction is considered, thus the term with respect to the tangential traction in Equation (3) vanishes. The influence function is determined by

$$A_{zz}(R) = \{(1 - \nu)/(\pi G)\} R^{-1} \quad (4)$$

where ν is Poisson ratio, G is the combined shear modulus of the two contact bodies which reads $1/G = 1/2(1/G_1 + 1/G_2)$, G_1 and G_2 are the shear modulus of the two contact bodies respectively. R is the distance between the response point and the impulse point.

A contact patch takes place where the surfaces of the two contact bodies coincide. The contact pressure can be computed according to the contact condition for the normal contact problems,

$$p_{Iz} = 0, \text{ the element is outside of the contact patch} \quad (5)$$

$$A_{IzJz} p_{Jz} + h_I = 0, \text{ the element is in contact} \quad (6)$$

When the normal force F_z is prescribed, then the following relationship must be satisfied,

$$F_z = Q \sum_I p_{Iz} \quad (7)$$

where Q is the area of an element.

2.3. Assessment strategy

As previously mentioned, the Hertz theory and the Kalker's theory are considered as representative half-space-based methods. The FE method is used to evaluate their applicability. The results of evaluation can be extended to other half-space-based methods. In the Kalker's theory, the potential contact region is divided into a number of square elements of equal size. To ensure a fair comparison with the FE method, the element size in the Kalker's theory is set equal to that in the zone of interest in the FE model, which is 0.31 mm.

To make this study more general and to facilitate the comparison between the Hertz theory, the Kalker's theory and the FE method, the FE solution is normalized with respect to the solutions of the Hertz theory and the Kalker's theory. The normalization is performed using critical values such as the maximum contact pressures (p_0 and p_{k0}) and the semi-axes of the contact patch (a_0 and a_k in the x direction, b_0 and b_k in the y direction) that are obtained from the Hertz theory and the Kalker's theory, respectively. The FE solution is treated as the reference. The deviations of the solutions of the half-space-based methods from the results of the FE method are therefore investigated.

In addition, contact patch eccentricity (b_0/a_0) is one important parameter that is related to the accuracy of half-space-based methods. This eccentricity depends on the ratio of the relative principal curvatures of the contact bodies. Therefore b_0/a_0 is varied by choosing various combinations of the principal radii of the curvature of the contact bodies. Using the real sizes of a wheel and a rail generates a contact patch with an eccentricity of 0.75. The value of b_0/a_0 lies in the range 0 to 1.00. Three other values in this range (0.20, 0.50 and 1.00) are also investigated to study the effects of the contact patch eccentricity.

3. Simulation results

In this study, frictional effects are not included. Therefore, only normal contact behaviors are evaluated, including the contact pressure distribution as well as the shape and the size of the contact patch. The influence of the significant dimension is investigated by varying a single dimension (e.g. height) while keeping the other dimensions (e.g. width and length) constant.

3.1. Normal solution when $b_0/a_0 = 0.75$

The cylindrical contact with a contact patch eccentricity of 0.75 is investigated in detail, and the results are presented in Table 1. In total, nine different combinations of significant dimensions of the contact body in terms of height, width and length are modeled. The contact patch for each combination is elliptical in shape, as shown in Fig. 4. The parameters a and b denote the semi-axes of the contact patch in the x and y directions, respectively.

Each normalized normal solution obtained using the FE method includes the normalized size of the contact patch and the maximum normalized contact pressure. A normalized value of 1.0 implies that the corresponding half-space-based solution matches the FE solution. It is observed that the values are not 1.0, which means that some differences do exist between the FE method and the two half-space-based methods. Possible causes include the finite dimension effect accounted for in the FE method, and numerical discretization.

Regarding the computed contact patch sizes, the maximum difference between the two half-space-based solutions and the FE solution is 3%, which is observed for the minor semi-axis b/b_k when comparing the FE method with the Kalker's theory. Moreover, Table 1 shows that the size of the contact patch is not affected by various combinations of significant dimensions. This finding suggests that the differences between the FE method and the half-space-based methods are due to the numerical discretization only. The corresponding error is up to 3% when the contact patch size is considered. The Hertz theory is an analytical approach, thus no numerical discretization process is involved. The Kalker's theory and the FE method involve numerical discretization, but the processes are different. For instance,

nodes are located at the centers of the elements in the Kalker's theory, whereas the nodes are located at the corners of the elements in the FE method.

Regarding the maximum normalized contact pressures (p_{max}/p_{k0} and p_{max}/p_0), their values are not equal to 1.0. This suggests that the FE method and the half-space-based methods predict different pressures. Among the nine combinations of significant dimensions, the case with a height of $h/2b_0 = 0.4$ and a width of $w/2b_0 = 8.0$ is the closest one to the half-space assumption. The corresponding pressure is 1.010, which indicates a difference of 1% in pressure between the FE method and the half-space-based methods. This difference is caused by numerical discretization. When the height is increasing to 4.0 and the width is decreasing to 1.1, the pressure increases by 3% from 1.010 to 1.040. This increase is caused by the finite dimension effect accounted for in the FE model. In other words, the half-space assumption introduces an error up to 3% in the maximum pressure compared with the FE method.

Table 1. FE solutions for static normal contact for each combination of significant dimensions.

Dimensions of lower body		Size of contact patch						Maximum pressure	
Height	Width	Major semi-axis		Minor semi-axis		Area		p_{max}/p_0	p_{max}/p_{k0}
$h/2b_0$	$w/2b_0$	a/a_0	a/a_k	b/b_0	b/b_k	A/A_0	A/A_k		
0.4	1.1	1.001	1.002	0.995	0.970	0.996	0.972	1.024	1.024
	2.0	1.001	1.002	0.995	0.970	0.996	0.972	1.010	1.010
	8.0	1.001	1.002	0.995	0.970	0.996	0.972	1.010	1.010
1.0	1.1	1.001	1.002	0.995	0.970	0.996	0.972	1.040	1.040
	2.0	1.001	1.002	0.995	0.970	0.996	0.972	1.010	1.010
	8.0	1.001	1.002	0.995	0.970	0.996	0.972	1.010	1.010
4.0	1.1	1.001	1.002	0.995	0.970	0.996	0.972	1.040	1.040
	2.0	1.001	1.002	0.995	0.970	0.996	0.972	1.010	1.010
	8.0	1.001	1.002	0.995	0.970	0.996	0.972	1.010	1.010

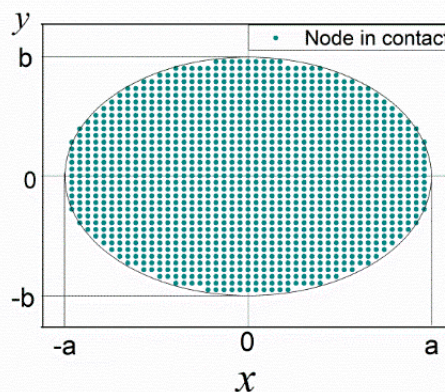


Fig. 4. Elliptical contact patch predicted by the FE method.

Fig. 5 shows the normalized contact pressure distributions along the longitudinal axis, as computed by the Hertz theory, the Kalker's theory and the FE method, for the most critical height of 4.0 and the width varying at 1.1, 2.0, and 8.0. All curves are Hertzian-type symmetric parabolas. This plot suggests that the half-space-based methods agree well with the FE method regarding the pattern of the pressure distribution.

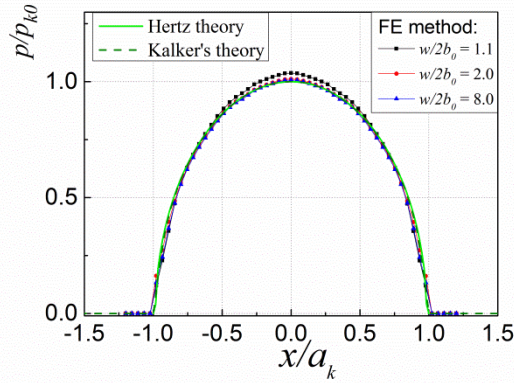


Fig. 5. Normalized contact pressure distributions along the longitudinal direction when $h/2b_0 = 4.0$.

3.2. Influence of the contact patch eccentricity b_0/a_0

The findings presented in the previous section are obtained based on a constant ratio of the principal radii of the cylindrical contact bodies, with the corresponding contact patch eccentricity of $b_0/a_0 = 0.75$. In this section, the ratio of the principal radii of cylindrical bodies is varied, with the resulting contact patch eccentricities of $b_0/a_0 = 0.20, 0.50, 0.75$, and 1.00 . The most critical combination of significant dimensions is examined, that is, a height of $h/2b_0 = 4.0$ and a width of $w/2b_0 = 1.1$. The calculated contact patch sizes and maximum pressures are given in Table 2. The largest deviation is observed when the contact patch eccentricity b_0/a_0 is 0.20 , and the major semi-axes a/a_0 is in question. The difference is up to 9%. It consists of contributions from both the numerical discretization and the finite dimension effect. This finding suggests that the deviation of the half-space-based methods from the FE method is dependent on the contact geometry, i.e. the ratio of the principal radii of the contact bodies. However, the possible deviation is limited to 9% in all cases.

Table 2. FE solutions for static normal contact for various contact patch eccentricities when the contact body geometry is cylindrical.

Eccentricity of contact patch	Dimensions of lower body		Sizes of contact patch			Maximum pressure
	Height	Width	Major semi-axis	Minor semi-axis	Area	
b_0/a_0	$h/2b_0$	$w/2b_0$	a/a_0	b/b_0	A/A_0	p_{max}/p_0
0.20	4.0	1.1	1.090	0.940	1.034	0.980
0.50	4.0	1.1	1.040	0.997	1.037	1.015
0.75	4.0	1.1	1.001	0.995	0.996	1.040
1.00	4.0	1.1	0.983	0.963	0.946	1.063

3.3. Influence of the contact body shape

Two cylindrical contact bodies with arbitrary principal radii were considered in the previous section. In this section, the investigation is extended to the contact between two non-cylindrical bodies with arbitrary principal radii. The resulting contact patches carry varying

eccentricities of $b_0/a_0 = 0.20, 0.50, 0.75$ and 1.00 . The most critical combination of significant dimensions, i.e. a height $h/2b_0 = 4.0$ and a width $w/2b_0 = 1.1$, is studied.

The calculated contact patch sizes and maximum pressures are given in Table 3. Comparing Table 3 with Table 2, it is found that all corresponding results are very close to each other, although some slight differences exist. It is concluded that the deviation of the half-space-based methods from the FE method is no greater than 9% even when the contact bodies are not cylindrical.

Table 3. FE solutions for various contact patch eccentricities when the contact geometry is arbitrary.

Eccentricity of contact patch	Dimensions of lower body		Sizes of contact patch			Maximum pressure
	Height	Width	Major semi-axis	Minor semi-axis	Area	
b_0/a_0	$h/2b_0$	$w/2b_0$	a/a_0	b/b_0	A/A_0	p_{max}/p_0
0.20	4.0	1.1	1.090	0.907	1.000	0.980
0.50	4.0	1.1	1.040	0.997	1.037	1.020
0.75	4.0	1.1	1.009	1.014	1.024	1.023
1.00	4.0	1.1	1.000	0.968	0.968	1.070

4. Discussions

In this study, the contact patch sizes and the normal pressures predicted by the FE method are regarded as accurate and are used to assess the performance of half-space-based methods. However, the FE solutions may also carry some errors due to numerical discretization and therefore may deviate from reality. These numerical errors can either exaggerate or cancel out the differences between the half-space-based solutions and the FE solutions. It is important to keep this in mind when comparing the half-space-based methods with the FE method.

An idealized contact problem involves contact bodies with infinite dimension. The contact stresses in the contact bodies form a certain distribution at and near the contact location but vanish at infinity. However, in reality, all contact bodies have finite dimensions; therefore, the contact stress distribution deviates from the idealized situation because of boundaries at finite distances. When these boundaries move toward the contact location, i.e. as the significant dimensions decrease, their influence on the stresses is increasing. In half-space-based methods such as the Hertz theory and the Kalker's variational theory, the contact stresses are computed without taking into account the influences of these finite-distance boundaries. Therefore, their predictions may increasingly deviate from reality as the significant dimensions approaches the size of the contact patch. Despite this drawback, such methods have gained popularity for solving non-conforming contact problems with finite dimensions, as long as the significant dimensions of the contact bodies are at least 3x times larger than the characteristic size of the contact patch. This study indicates that this limit can be reduced to 1.1x times larger under the condition that a deviation of up to 9% introduced by the half-space assumption can be accepted (see Fig. 6). This conclusion is valid for most ratios of the relative principal radii of arbitrarily shaped contact bodies.

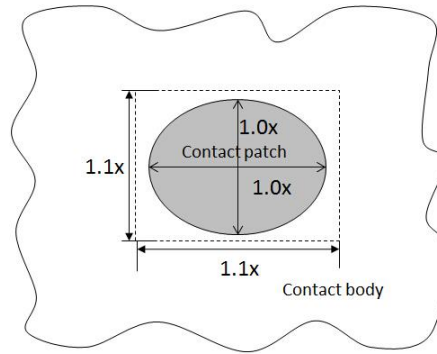


Fig. 6. Significant dimensions of the contact bodies and characteristic size of the contact patch (top view).

The simulations presented in this study consider Hertzian non-conforming contacts between two arbitrary geometric bodies. The findings discussed above should also apply for the following types of contacts.

- 1) In the numerical simulations, specific chosen values were assigned to the dimensions of the contact bodies, the load and the material properties. When those values are scaled, the findings should remain valid as long as the contact problems in question remain linear elastic in nature and the deformation is small. This self-similarity rule is explained in [21, 22].
- 2) Although the simulations presented in this study consider Hertzian contact, the findings should also apply to some non-Hertzian elastic contacts, excluding conforming contacts. A typical non-Hertzian contact is the two-point contact between a wheel and a rail at the rail crossing nose [23, 24], as shown in Fig. 7(a). This type of contact problems results in two contact patches. For stress calculations using half-space-based methods, this problem may be decomposed into two individual contact problems at each point, as illustrated in Fig. 7(b). The part of the contact body in the vicinity of each contact point is considered as a local contact body. If each individual contact is of the Hertzian type and the significant dimension of each local contact body in the vicinity of the resulting contact patch satisfies the 1.1x condition, then the findings of this study can be extended to the original two-point non-Hertzian contact. A more general type of non-Hertzian contact is a multi-point contact such as that shown in Fig. 7(c). Provided that the 1.1x condition is satisfied for each individual contact problem, the decomposition technique can again be applied. Therefore the findings can be extended to a multi-point contact as well.

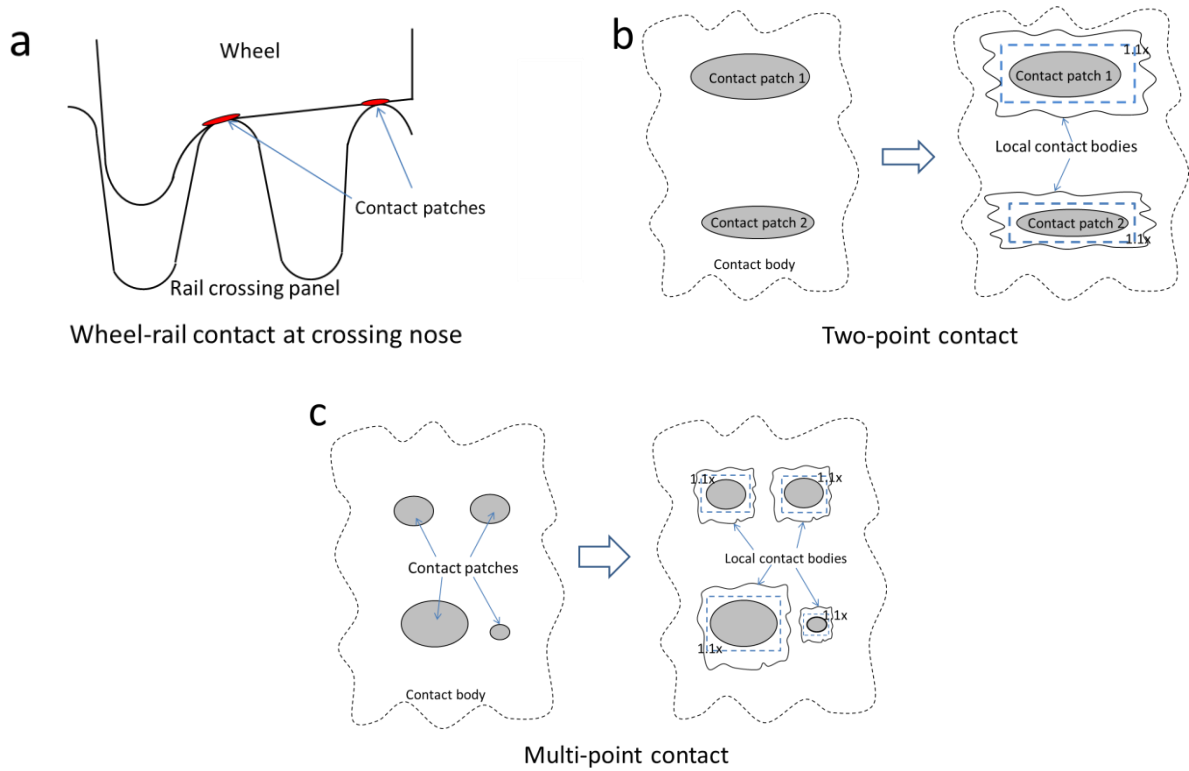


Fig. 7. Schematic diagrams of: (a) A wheel-rail contact at the rail crossing nose with two contact patches, a typical non-Hertzian contact problem; (b) Each contact patch satisfies the 1.1x condition and thus the non-Hertzian problem of (a) may be decomposed into two Hertzian problems; (c) A general multi-point contact and the decomposition.

3) Although this study was implemented using static normal contact examples, the findings can also be applied to the case of a steady state rolling contact without traction. This is because the normal solution for static contact problems is equivalent to that for a steady state pure rolling contact problem. This equivalence can be seen from the identical normal solutions obtained for these two types of contact problems using the Kalker's theory. In practice, lubrication is widely applied to rolling components, such as bearings, to reduce the traction transmitted at the contact interface. Therefore these findings are also valid for most lubricated rolling contact problems. However, for a case in which the traction is too high to be ignored, the applicability of half-space-based methods for obtaining the tangential solution requires further investigation.

5. Conclusions

In this paper, the FE method is used to assess the applicability of half-space-based methods to normal contact problems. Different combinations of significant dimensions of the contact bodies in terms of height, width, and length are studied. Various contact patch eccentricities are considered. Both cylindrical and non-cylindrical contact geometries are examined. The scenarios considered effectively cover the entire range of interest from the nearly smallest possible significant dimension (1.1x the characteristic size of the contact patch) to infinite

dimension. Based on the observations from the numerical experiments and the analysis and the discussions, the following conclusions can be drawn.

Half-space-based methods can deliver reasonable accurate solutions for most non-conforming elastic contact problems, as long as the significant dimensions of the contact bodies are 1.1x larger than the characteristic size of the contact patch. The corresponding error is within 9%.

This new finding broadens the applicability of half-space-based methods, and lends greater confidence to studies of contact problems in mechanical engineering where half-space-based methods are applied. In engineering practice, this study can be a guide to assist engineers in choosing appropriate methods when solving contact problems. Should the 1.1x conditions be satisfied and an error tolerance of 9% be acceptable, the half-space-based methods are preferred, as they are relatively easier to apply and more computationally efficient. Otherwise, the FE method should be considered [24].

References

- [1] Johnson KL. *Contact mechanics*. Cambridge: Cambridge university press; 1987.
- [2] Sadeghi F, Jalalahmadi B, Slack TS, Raje N, Arakere NK. A review of rolling contact fatigue. *J Tribol* 2009;131:041403.
- [3] Hertz H. Über die berührung fester elastische Körper und über die Harte. *Journal fur die reine und angewandte Mathematik* 1882;92:156-71.
- [4] Carter FW. On the action of a locomotive driving wheel. *Proc R Soc London, Ser A* 1926;112:151-7.
- [5] Johnson KL. Tangential traction and microslip in rolling contact. In: Bidwell JR, editor. *Rolling contact phenomena*. Amsterdam: Elsevier; 1962. p. 6-28.
- [6] Kalker JJ. *Three-dimensional elastic bodies in rolling contact*. Dordrecht, The Netherlands: Kluwer Academic Publishers; 1990.
- [7] Wiest M, Kassa E, Daves W, Nielsen JCO, Ossberger H. Assessment of methods for calculating contact pressure in wheel-rail/switch contact. *Wear* 2008;265:1439-45.
- [8] Bhushan B. Contact mechanics of rough surfaces in tribology: multiple asperity contact. *Tribol Lett* 1998;4:1-35.
- [9] Rajendrakumar PK, Biswas SK. Elastic contact between a cylindrical surface and a flat surface — a non-Hertzian model of multi-asperity contact. *Mech Res Commun* 1996;23:367-80.
- [10] Harris TA. *Rolling bearing analysis*. New York: John Wiley and sons; 2001.
- [11] Yoffe E. Modified Hertz theory for spherical indentation. *Philosophical Magazine A* 1984;50:813-28.
- [12] Wu S-H, Tsai S-J. Contact stress analysis of skew conical involute gear drives in approximate line contact. *Mech Mach Theory* 2009;44:1658-76.
- [13] Kalker J. Survey of wheel—rail rolling contact theory. *Veh Syst Dyn* 1979;8:317-58.
- [14] Chan SK, Tuba IS. A finite element method for contact problems of solid bodies—part I. Theory and validation. *Int J Mech Sci* 1971;13:615-25.
- [15] Zhao X, Li Z. The solution of frictional wheel—rail rolling contact with a 3D transient finite element model: Validation and error analysis. *Wear* 2011;271:444-52.

- [16] Yan W, Fischer FD. Applicability of the Hertz contact theory to rail-wheel contact problems. *Arch Appl Mech* 2000;70:255-68.
- [17] Wriggers P. Finite element algorithms for contact problems. *Archives of Computational Methods in Engineering* 1995;2:1-49.
- [18] Li Z. Wheel-rail rolling contact and its application to wear simulation (Ph.D. thesis). Delft, The Netherlands: Delft University of Technology; 2002.
- [19] Boussinesq J. Application des potentiels à l'étude de l'équilibre et du mouvement des solides élastiques. Paris: Gauthier-Villars; 1885.
- [20] Cerruti V. *Accademia dei Lincei. Roma Mem fis mat* 1882.
- [21] Barber JR. *Elasticity*. Kluwer: Springer; 1992.
- [22] Borodich FM. Similarity in the problem of contact between elastic bodies. *Journal of Applied Mathematics and Mechanics* 1983;47:440-2.
- [23] Kassa E, Andersson C, Nielsen JC. Simulation of dynamic interaction between train and railway turnout. *Vehicle System Dynamics* 2006;44:247-58.
- [24] Wei Z, Shen C, Li Z, Dollevoet R. Wheel–Rail Impact at Crossings: Relating Dynamic Frictional Contact to Degradation. *Journal of Computational and Nonlinear Dynamics* 2017;12:041016-11.